Availability of activated CD4+ T cells dictates the level of viremia in naturally SIV-infected sooty mangabeys

Nichole R. Klatt,[1,2] Francois Villinger,[2,3] Pavel Bostik,[3] Shari N. Gordon,[1,2] Lara Pereira,[3] Jessica C. Engram,[1] Ann Mayne,[3] Richard M. Dunham,[1,2] Benton Lawson,[2] Sarah J. Ratcliffe,[4] Donald L. Sodora,[5] James Else,[2] Keith Reimann,[6] Silvija I. Staprans,[7] Ashley T. Haase,[8] Jacob D. Estes,[9] Guido Silvestri,[1,2] and Aftab A. Ansari[2,3]

[1]Department of Pathology and Laboratory Medicine, University of Pennsylvania School of Medicine, Philadelphia, Pennsylvania, USA. [2]Yerkes National Primate Research Center and [3]Department of Pathology and Laboratory Medicine, Emory University, Atlanta, Georgia, USA. [4]Department of Biostatistics and Epidemiology, University of Pennsylvania School of Medicine, Philadelphia, Pennsylvania, USA. [5]Department of Internal Medicine and Department of Microbiology, University of Texas Southwestern Medical Center, Dallas, Texas, USA. [6]Beth Israel Deaconess Medical Center, Harvard Medical School, Boston, Massachusetts, USA. [7]Merck Vaccines, West Point, Pennsylvania, USA. [8]Department of Microbiology, University of Minnesota, Minneapolis, Minnesota, USA. [9]AIDS and Cancer Virus Program, Science Applications International Corporation, National Cancer Institute, Frederick, Maryland, USA.

Naturally SIV-infected sooty mangabeys (SMs) remain asymptomatic despite high virus replication. Elucidating the mechanisms underlying AIDS resistance of SIV-infected SMs may provide crucial information to better understand AIDS pathogenesis. In this study, we assessed the determinants of set-point viremia in naturally SIV-infected SMs, i.e., immune control of SIV replication versus target cell limitation. We depleted CD4+ T cells in 6 naturally SIV-infected SMs by treating with humanized anti-CD4 mAb (Cdr-OKT4A-huIgG1). CD4+ T cells were depleted almost completely in blood and BM and at variable levels in mucosal tissues and LNs. No marked depletion of CD14+ monocytes was observed. Importantly, CD4+ T cell depletion was associated with a rapid, significant decline in viral load, which returned to baseline level at day 30–45, coincident with an increased fraction of proliferating and activated CD4+ T cells. Throughout the study, virus replication correlated with the level of proliferating CD4+ T cells. CD4+ T cell depletion did not induce any changes in the fraction of Tregs or the level of SIV-specific CD8+ T cells. Our results suggest that the availability of activated CD4+ T cells, rather than immune control of SIV replication, is the main determinant of set-point viral load during natural SIV infection of SMs.

Introduction

The HIV epidemic in humans arose after zoonotic transmission of simian CD4+ T cell tropic lentiviruses, which naturally infect a range of African monkey host species and are now collectively known as SIVs (1). HIV-1 arose after cross-species transmission of SIVcpz, which naturally infects chimpanzees (*Pan troglodytes*), while HIV-2 arose from transmission of SIVsmm, which naturally infects sooty mangabeys (SMs, *Cercocebus torquatus atys*) (2). SIVsmm is also the likely source of pathogenic SIVmac strains that are commonly used to infect rhesus macaques (*Macaca mulatta*) (3, 4).

Natural SIVsmm infection of SMs is common both in the wild and in captivity and often correlates with sexual maturity (5). In stark contrast to HIV-infected humans, who almost invariably progress to AIDS if they are not treated, naturally SIV-infected SMs usually maintain normal CD4+ T cell counts and very rarely progress to AIDS, despite chronic high levels of viral replication (6–10). The mechanisms by which these animals remain healthy despite levels of virus replication that are associated with AIDS in non-naturally adapted species (i.e., humans and macaques) have yet to be completely defined. However, it is now widely recognized that understanding the AIDS resistance of natural SIV hosts will provide important clues to AIDS pathogenesis (11, 12).

SIVsmm infection of SMs is associated with levels of viral replication that are as high as, or even higher than, those observed in pathogenic HIV infection of humans (6, 7, 9). The fact that SMs maintain high viral load indicates that the disease resistance of these animals is unlikely to be because of particularly strong SIV-specific CTL responses. This hypothesis is also supported by the observations that SIV-infected SMs have lower levels of virus-specific T cell responses than do HIV-infected individuals (13) and that depletion of CD8+ T cells does not result in any significant increase in virus replication (14). Similar to pathogenic models of HIV/SIV infection (15–18), more than 90% of SIVsmm replication in naturally SIV-infected SMs occurs in short-lived cells, which suggests that activated CD4+ T cells are the major site for viral replication (19). The fact that CD4+ T cells are the main targets of SIVsmm replication is also confirmed by the observation that mucosal CD4+ T cells are rapidly depleted during acute SIVsmm infection of SMs (20). However, despite destruction of mucosal CD4+ T cells during acute infection and subsequent development of chronic viremia, SMs infected with SIVsmm remain healthy and rarely experience declining peripheral CD4+ T cell counts (8). While the mechanisms responsible for the preservation of normal CD4+ T cell counts in SIV-infected SMs are still unclear, many reports indicate that a striking and consistent feature of this model of infection is the lack of generalized immune activation

Nonstandard abbreviations used: BAL, bronchoalveloar lavage; IHC, immunohistochemistry; RB, rectal biopsy; SM, sooty mangabey.

Conflict of interest: The authors have declared that no conflict of interest exists.

Citation for this article: *J. Clin. Invest.* **118**:2039–2049 (2008). doi:10.1172/JCI33814.

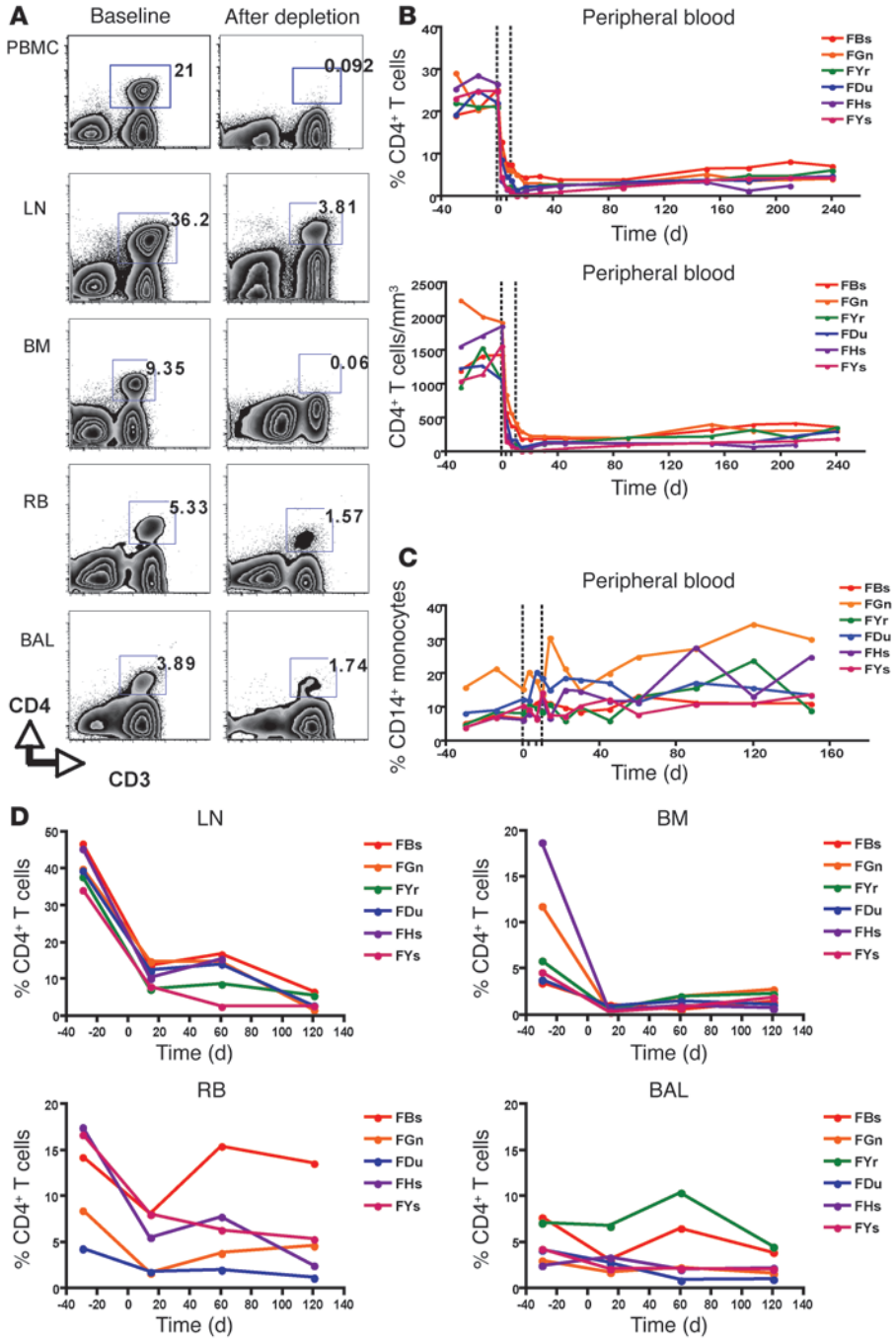

Figure 1
In vivo CD4+ T cell depletion in SIV-infected SMs. (**A**) Representative flow cytometric contour plots (*x* axis, CD3; *y* axis, CD4) of CD4+ T cells in PBMCs, LNs, BM, RBs, and BAL at 30 d before depleting antibody treatment and nadir CD4+ T cell fraction (10–14 d) after depleting antibody treatment was initiated. Numbers denote percentage of cells within the boxed regions. (**B**) Longitudinal assessment of the percent and absolute number of CD3+CD4+ T cells for each animal through 240 d after depletion. (**C**) Longitudinal assessment of the percent of circulating CD14+ monocytes for each animal through 150 d after depletion. Depleting anti-CD4 Ab was administered at 0, 3, 7, and 10 d (represented by tick marks and dotted lines). (**D**) Longitudinal assessment of the percent of CD3+CD4+ T cells in LNs, BM, RBs, and BAL at –30, 14, 60, and 120 d.

(6, 8, 21), one of the major correlates of disease progression in pathogenic models (22–24).

One question regarding natural SIV infection of SMs is: What are the determinants of the set-point level of viremia in these animals? Particularly, what is the role of immune control of SIV infection versus target cell limitation, and in this context, what is the specific role of CD4+ T cells (i.e., providing targets for virus replication versus helping SIV-specific humoral and cellular immune responses) in this nonpathogenic model of infection? A more detailed study of the determinants of viremia during natural SIV infection of SMs may contribute to our understanding of how these animals remain disease-free in the face of highly replicating SIV.

To further understand the role of CD4+ T cells in determining set-point viremia during SIV infection of SMs, we treated 6 animals with repeated infusion of the humanized anti-CD4 monoclonal antibody Cdr-OKT4A-huIgG1 (referred to herein as OKT4A), causing major depletion of these cells in vivo, and longitudinally measured a number of virological and immunological parameters. We observed that CD4+ T cell depletion was consistently associated with a rapid and significant decrease (2–3 logs) in viral load, suggesting that CD4+ T cells have a limited direct effect on facilitating immune control of SIV replication. Within a few weeks of initiation of the depleting treatment, viral loads returned to baseline levels, coincident with a marked increase in the fraction of

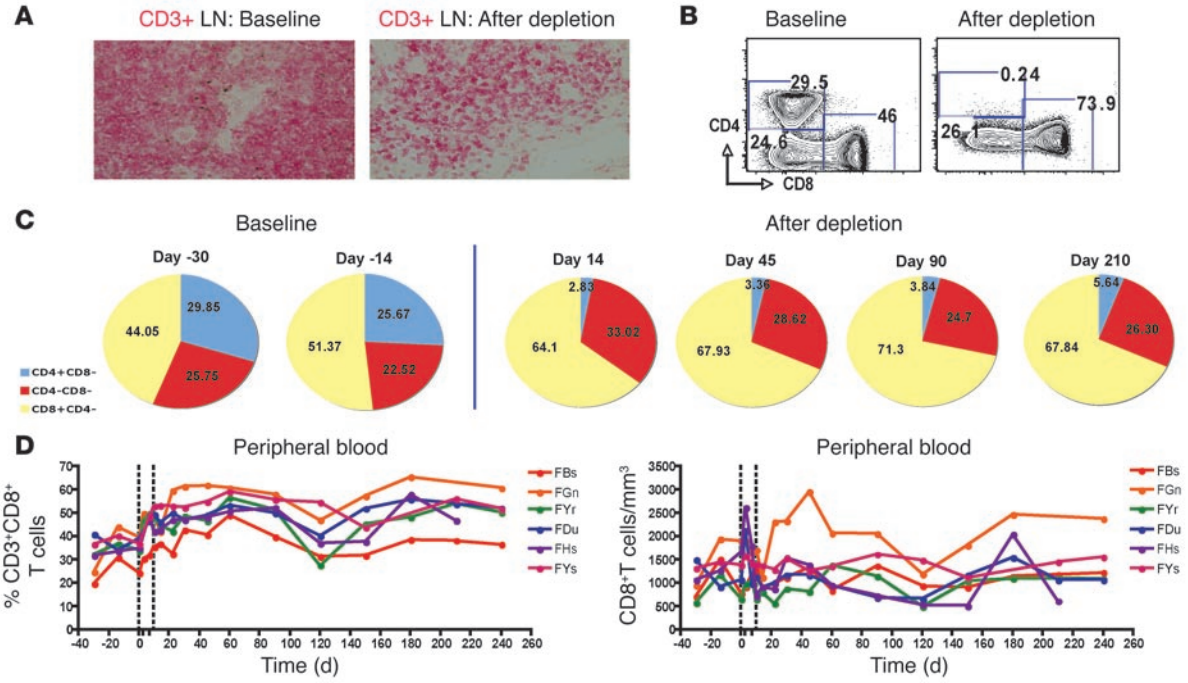

Figure 2

The observed decline of CD4+ T cells is the result of a true depletion of CD4+ T cells, not of masking by the depleting antibody. (**A**) CD3+ T cells in the paracortical region of the LNs were stained by IHC at baseline (–30 d) and 14 d after depletion. (**B**) Representative contour plot of gating strategy for the analyzed CD3+ T cell subsets: $CD4^+CD8^-$, $CD4^-CD8^+$, and $CD4^-CD8^-$ (*x* axis, CD8; *y* axis, CD4). Numbers denote percentage of cells within the boxed regions. (**C**) Longitudinal assessment of the fractions of $CD4^+CD8^-$, $CD4^-CD8^-$, and $CD8^+CD4^-$ CD3+ T cells by flow cytometry (average of 6 animals represented). Numbers denote percentage of cells in the indicated subset. (**D**) Longitudinal assessment of the percent and absolute number of CD8+ T cells (gated on CD3+ lymphocytes) through 240 d after depletion. Dotted lines and tick marks represent CD4-depleting antibody treatment.

activated and proliferating CD4+ T cells (even in the context of a persistent CD4+ T cell depletion). The fact that the level of CD4+ T cell activation correlated with plasma viremia throughout the study is compatible with a model in which the availability of activated CD4+ T cells as targets for SIV is the main determinant of the prevailing level of virus replication in SIV-infected SMs.

Results

Treatment with anti-CD4 mAb resulted in substantial CD4+ T cell depletion in the blood, LNs, and mucosa-associated lymphoid tissue. To investigate the in vivo role of CD4+ T cells in determining set-point viremia during natural SIV infection of SMs, we depleted CD4+ T cells as described in Methods. The level of CD4+ T cell depletion in each of the tissues examined was assessed by multicolor flow cytometry (Figure 1A). Prior to administration of the anti-CD4 antibody, the baseline fraction of $CD3^+CD4^+$ T cells was 24.95% ± 3.44%, with an absolute CD4+ T cell number of 1,550.3 ± 392.2 cells/mm^3 (mean ± SD; Figure 1B). Immediately after the administration of the depleting antibody, a reduction in CD4+ T cells was observed. At the nadir, between 10 and 14 d, CD4+ T cells were depleted on average 95.18% in peripheral blood, and residual CD4+ T cells constituted 1.55% ± 1.41% of CD3+ T lymphocytes (mean ± SD), with an average absolute count of 46.28 cells/mm^3 (Figure 1B). In each of the 6 SIV-infected SMs, the antibody-mediated depletion of CD4+ T cells was persistent, with average levels below 7% of total T lymphocytes at 8 months after depletion (i.e., CD4+ T cell reconstitution less than 15% that of baseline). This slow repopulation of CD4+ T cells did not appear to be simply an effect of SIV infection, because CD4-depleted, SIV-uninfected SMs also showed relatively inefficient reconstitution of their CD4+ T cell pools (see Supplemental Figures 1 and 2; supplemental material available online with this article; doi:10.1172/JCI33814DS1), particularly compared with the kinetics of CD8+ T cell repopulation after antibody-mediated depletion (14, 25–27). However, the pace of CD4+ T cell reconstitution was somewhat faster in the uninfected animals, which suggests that SIV infection had a negative effect on the homeostasis of CD4+ T cells. Interestingly, the rebound of CD4+ T cell proliferation observed after depletion in the SIV-infected SMs was also observed in the uninfected animals. Importantly, both infected and uninfected SMs tolerated CD4+ T cell depletion without any detectable adverse reaction or signs of AIDS throughout the postdepletion observation period (>18 mo). These findings are interesting because CD4+ T cell levels below 100 cells/mm^3 are associated with high risk of developing AIDS in both HIV-infected humans and SIV-infected macaques.

We next assessed the level of CD4+ T cells in various tissues by conducting LN biopsies, rectal biopsies (RBs), bronchoalveolar lavages (BALs), and BM aspiration and measuring the fraction of CD4+ T cells by immunophenotyping via flow cytometry. Variable levels of CD4+ T cell depletion were observed in the tissues examined (Figure 1, A and D). The effect of anti-CD4 antibody was most pronounced in LN and BM aspiration (CD4+ T cell depletion of 90.2% ± 4.61% and 89.3% ± 12.12% of baseline, respectively) and less marked in mucosal tissues (CD4+ T cell depletion of 60.2% ± 14.4%

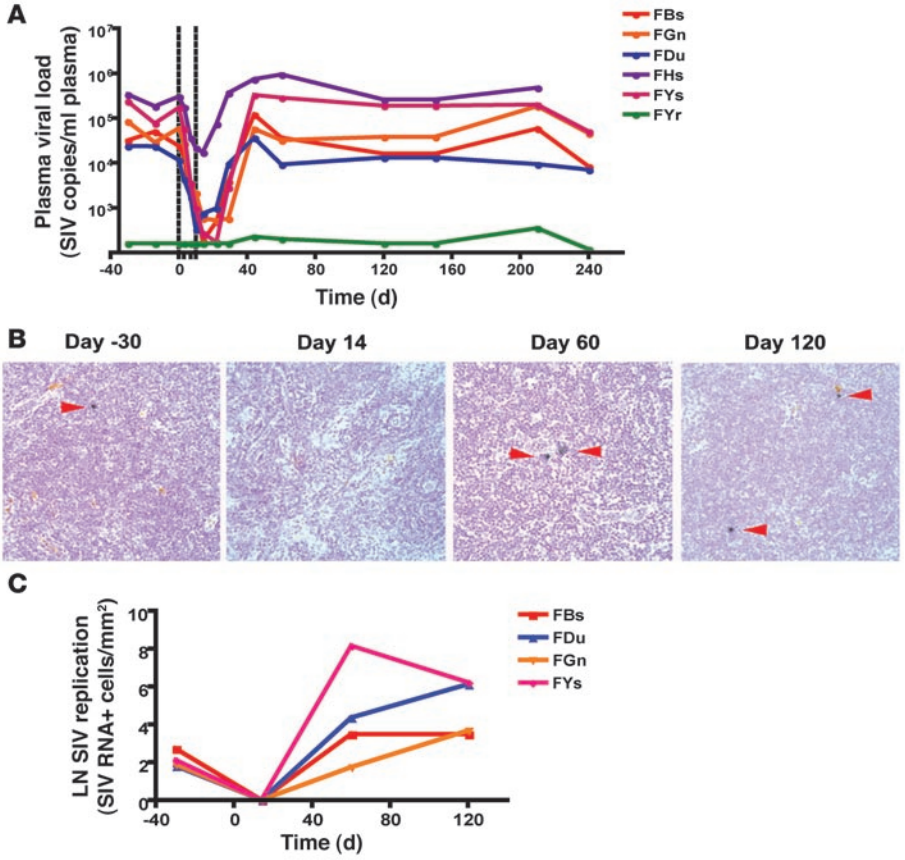

Figure 3
CD4⁺ T cell depletion is associated with a decline of viremia in SIV-infected SMs. (**A**) Longitudinal assessment of SIV plasma viral load (SIV copies/ml plasma by RT-PCR) for each animal through 240 d after depletion. Dotted lines and tick marks represent CD4-depleting antibody treatment. (**B** and **C**) In situ hybridization demonstrated SIV RNA⁺ productively infected cells were uniformly located within the T cell zone of LNs both prior to CD4⁺ T cell depletion (–30 d) and following the reemergence of CD4⁺ T cells after treatment (60 and 120 d), but were absent concurrent to loss of plasma viremia (14 d).

and 44.7% ± 21.46% of baseline in RB and BAL, respectively; mean ± SD; Figure 1D). The less severe depletion observed in mucosal tissues may be the result of a relative lack of distribution of the depleting antibody. Interestingly, the nadir of CD4⁺ T cell depletion in LNs was observed at 120 d, much later than in other tissues, and at a time when presumably little to no OKT4A depleting antibody is present in the circulation, which suggests that CD4⁺ T cells are perhaps being mobilized and leaving LNs in an attempt to repopulate the other CD4⁺ T cell–depleted compartments. To investigate a possible depletion of CD4⁺ monocytes/macrophages, we also monitored the frequency and absolute number of CD14⁺ cells. As shown in Figure 1C, the level of CD14⁺ monocytes in peripheral blood, BM aspiration, and LNs remained substantially unchanged throughout the follow-up period. These results demonstrate that the anti-CD4 mAb effectively depleted most CD4⁺ T cells from peripheral blood, LNs, and BM and had a more limited, but still very apparent, effect in depleting CD4⁺ T cells from mucosal tissues.

The decline of CD4⁺ T cells is the result of true depletion of CD4⁺ T cells. In order to ensure that the animals experienced a genuine depletion of CD4⁺ T cells and not simply a masking of CD4 by the depleting antibody, we measured the levels of CD3⁺ T cells in the LNs by immunohistochemistry (IHC) and in peripheral blood by flow cytometry. We reasoned that if the OKT4A antibody was masking and not depleting, CD3⁺ T cell levels would be similar before and after depletion, while if the antibody was truly depleting, we would observe a net loss of CD3⁺ T cells. Indeed, the fraction of CD3⁺ T cells in LNs was substantially reduced (Figure 2A), providing strong evidence that true depletion of CD4⁺ T cells in the LNs had occurred. In addition, we longitudinally measured the relative fractions of circulating CD3⁺ T cell subsets and determined the frequencies of $CD4^+CD8^+$, $CD4^-CD8^+$, and $CD4^-CD8^-$ T cells. We reasoned that if the antibody had a prominent masking effect, there would be a rise in $CD3^+CD4^-CD8^-$ T cells. As shown in Figure 2, B and C, no selective increase in the $CD3^+CD4^-CD8^-$ subset was noted, indicating that the CD4⁺ T cells were indeed depleted from the lymphocyte populations as a result of treatment with anti-CD4 antibody. To further verify that the changes in lymphocyte fractions observed was caused by an expansion of the fraction — not the absolute number — of CD8⁺ T cells, we measured CD8⁺ T cells in the tissues collected. As shown in Figure 2D, treatment with the anti-CD4 mAb antibody resulted in an increase in the percentage of $CD3^+CD8^+$ T cells with no significant changes in the absolute number of these cells. Collectively, these data demonstrate that the loss of CD4⁺ T cells observed was the result of true depletion by the anti-CD4 antibody, not a masking effect.

CD4⁺ T cell depletion causes a rapid, but transient, decrease in viremia in naturally SIV-infected SMs. In order to determine the impact of CD4⁺ T cell depletion on viral replication in SIV-infected SMs, we next measured plasma viral load longitudinally throughout the study by RT-PCR as previously described (8). Figure 3A shows that following treatment with the anti-CD4 antibody, all animals that had detectable plasma viral load prior to depletion (5 of 6 SMs) manifested a rapid decrease in plasma viremia, with an average decline of approximately 2 logs between baseline and 14 d after depletion. A similar decline in the level of virus replication was observed when we assessed the level of SIV-RNA in LN tissues by in situ hybridization (Figure 3, B and C). Starting approximately 20 d after depletion, viral load showed a progressive increase, reaching baseline levels by 60 d (Figure

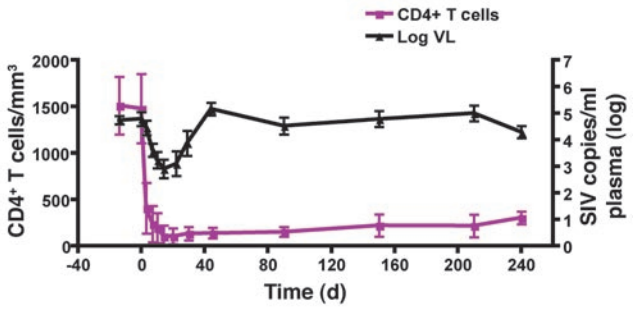

Figure 4
Relationship between viral load and absolute number of circulating CD4+ T cells. Longitudinal assessment of the average viral load (VL; black line, right axis) and average CD4+ T cell counts (purple line, left axis) for all animals except FYr. Error bars represent SEM.

3A). The kinetics of plasma viral load following CD4+ T cell depletion was confirmed by the analysis of virus replication in lymphoid tissues as detected by in situ hybridization (Figure 3, B and C).

The observation that depletion of CD4+ T cells was followed by a rapid decrease in viremia is consistent with the possibility that in this cohort of naturally SIV-infected SMs, the measured changes in virus replication are caused by decreased availability of target cells. Because one possible outcome of this study was that CD4+ T cell depletion would affect the CD4+ T cell–mediated immune control of viremia, our study cohort included the animal FYr, with baseline viral loads less than 160 copies/ml plasma, and animals FDu and FBs, with less than 5×10^4 copies/ml plasma. As seen in Figure 3A, viral load remained always under 400 copies/ml plasma in FYr; similarly, no increase in viremia as a result of CD4+ T cell depletion was noted in the other 2 SMs, consistent with the hypothesis that CD4+ T cells do not play a major role in controlling SIV replication in SMs. However, because the antibody used depleted SIV-specific CD4+ T cells as well as the targeted CD4+ cells, this result did not completely rule out the possibility that SIV-specific CD4+ T cells contribute to the low virus replication observed in these animals.

It is possible that the OKT4A CD4-depleting antibody might have direct antiviral effects by interference with binding of HIVenv to CD4, thus contributing to the decline in viremia (K. Reimann, unpublished observations). Examination of the decline after treatment in viremia levels does not elucidate the relative contribution of these 2 effects of the anti-CD4 antibody (i.e., depletion of CD4+ T cells versus direct antiviral effects). However, the correlation noted between plasma viral load and the level of activated/proliferating CD4+ T cells throughout the period after CD4 depletion — particularly at a time when no direct antiviral effect of the anti-CD4 antibody was observed (see below) — strongly suggests that the availability of target cells is the key determinant of virus replication in naturally SIV-infected SMs.

CD4+ T cell depletion is followed by an increase in CD4+ T cell activation and proliferation that correlates with viral load rebound. To better assess the relationship between the extent of CD4+ T cell depletion and level of virus replication, we carefully examined the kinetics of the absolute CD4+ T cell counts and plasma viral load at various time points after CD4+ T cell depletion (Figure 4). The decrease in viral load early after anti-CD4 administration was coincident with CD4+ T cell depletion. However, the rapid rebound of viral load was observed at 30–45 d, at a time when the absolute number of CD4+ T cells was still considerably lower than baseline. Log-transformed viral loads and CD4+ T cell counts during the depletion period were highly significantly correlated ($P < 0.0001$) via partial correlations. The partial correlation was adjusted for time and animal effects, with random effects models used to estimate the influence of time and animal on CD4+ T cell counts and log viral loads in the calculations. It should be noted that the performed analysis might have been influenced by the fact that the majority of time points were during the early stages after depletion, when the rapid declines of both CD4+ T cells and viremia were temporally associated.

Because primate lentiviruses preferentially replicate in activated and/or proliferating CD4+ T cells (11, 28), we next sought to determine whether the changes in viral replication observed in our cohort of naturally SIV-infected SMs after treatment with anti-CD4 antibody also correlated with the level of CD4+ T cell activation and/or proliferation. We first measured longitudinally the fraction of CD4+ T cells expressing the proliferation marker Ki67 (Figure 5A) and the activation markers CD69 (Figure 5A) and HLA-DR (data not shown) by flow cytometry. The nadir of CD4+ T cell levels was followed by a striking increase in the frequency of activated and proliferating CD4+ T cells: the average percentage of CD4+ T cells expressing Ki67 increased from 0.75% at baseline to 13.2% at the nadir of CD4 depletion (Figure 5B). The absolute numbers of CD4+Ki67+ T cells actually decreased from a predepletion level of 11.23 ± 5.07 cells/mm^3 to 4.28 ± 1.58 cells/mm^3 at the nadir (mean ± SD). However, as shown in Figure 5C, this decline in the absolute number of circulating CD4+Ki67+ T cells was followed by an increase at peak activation levels of up to 11.30 ± 3.61 cells/mm^3 (mean ± SD), strikingly similar to baseline. The fraction of activated CD4+ T cells expressing CD69 also increased dramatically, from an average of less than 1% CD4+CD69+ T cells before depletion to an average of 96.2% of CD4+ T cells at the nadir (Figure 5B). The observed increase of circulating CD4+CD69+ T cells may also reflect a more rapid and/or prominent egress of activated CD4+ T cells from the LNs. As expected, we observed an increase in the fraction of proliferating CD4+Ki67+ T cells in tissues after CD4+ T cell depletion that was temporally associated with the increase in plasma viral load (Figure 5D). We also investigated the relationship between viremia and the fraction of circulating and tissue-based CD4+CCR5+ T cells in our group of CD4+ T cell–depleted, SIV-infected SMs and found no significant correlation between these parameters (Supplemental Figure 3).

We next sought to directly assess the relationship between the frequency of activated or proliferating CD4+ T cells and the observed changes in viral load by performing the same partial correlation analysis that we performed for CD4+ counts and log viral loads by adjusting for time and animals. We found a significant direct correlation ($P < 0.0001$) between the number of CD4+Ki67+ T cells and viral load throughout the study period (Figure 5C). In contrast to the correlation between CD4+ T cell counts and viral load, which was more apparent during the early stages of depletion, the direct correlation between CD4+Ki67+ T cell number and viral load was evident throughout the study. This finding was further highlighted in the data for each individual animal (Figure 5D).

The finding of a direct correlation of both CD4+ T cell count and CD4+Ki67+ T cell count with plasma viremia strongly suggests that in naturally SIV-infected SMs, the number of both total and proliferating CD4+ target cells is a key determinant of the level of virus replication. Consistent with this notion is the observation that in SIV-infected SMs, most cells producing SIV are localized within clusters of CD3+ T cells, as detected by double-label in situ

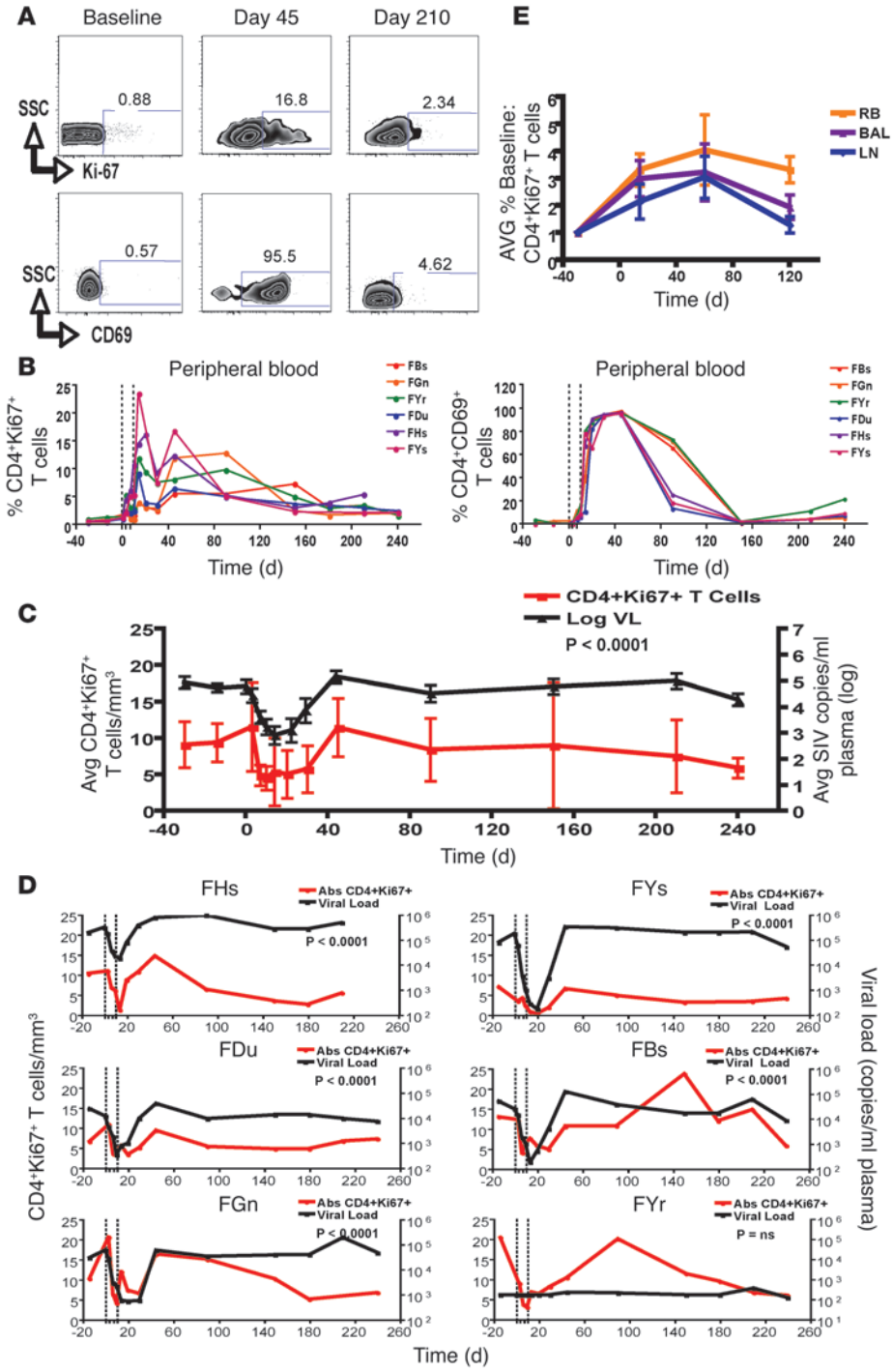

Figure 5
The level of activated/proliferating CD4+ T cells increases after CD4+ T cell depletion and correlates with viral load. (**A**) Representative flow cytometric plots of CD4+Ki67+ T cells and CD4+CD69+ T cells at baseline (14 d before depletion) and 45 and 210 d after depletion. SSC, side scatter. (**B**) Longitudinal assessment of the percent of CD4+Ki67+ T cells and CD4+CD69+ T cells in each animal through 240 d after depletion. (**C** and **D**) Longitudinal assessment of the viral load (black, right axis) and absolute number of CD4+Ki67+ T cells (red, left axis) averaged for all animals except FYr (**C**) and for each individual animal (**D**). A significant, direct correlation between the number of CD4+Ki67+ T cells and viral load was found when calculating all time points, except for FYr ($P < 0.0001$). (**E**) Longitudinal assessment of the average fraction of CD4+Ki67+ T cells plotted as fraction of baseline for RB, BAL, and LN.

hybridization/IHC techniques on sections of LNs and RB tissues, and rarely include CD68+ macrophages or CD11c dendritic cells (G. Silvestri, unpublished observations).

The CD4+ T cell proliferation increase after depletion is likely caused by homeostasis-driven mechanisms. The increased level of CD4+ T cell proliferation observed in our cohort of SIV-infected SMs after treatment with the depleting anti-CD4 antibody could be secondary to the selective activation of SIV-specific CD4+ T cells (likely in response to the rebound of virus replication) or by the activation of homeostatic (i.e., non–antigen-specific) mechanisms aimed at repopulating the CD4+ T cell pool. We sought to address this issue by longitudinally examining the diversity of TCR repertoire, with the expectation that CD4+ T cell proliferation driven by SIV would be reflected in an oligoclonal repertoire, less diverse than a truly homeostasis dependent proliferation. We sorted peripheral blood CD4+ T cells from each animal before and after depletion and determined the relative degree of TCR heterogeneity by TCR V-J fragment–specific Southern hybridization, as described previously (29). In these experiments, the signal obtained from the positive control ratio was denoted as 1 (i.e., 100% homology between the probe and target), and ratios less

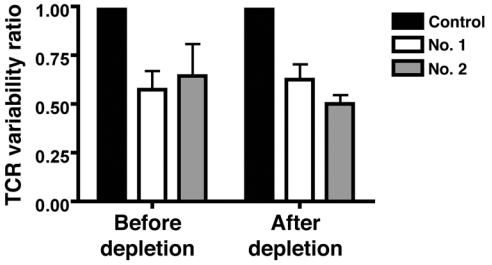

Figure 6
Analysis of TCR repertoire diversity via TCR V-J fragment–specific Southern hybridization. TCR V-J PCR amplicons were generated from 3 aliquots of $CD4^+$ T cells from each PBMC sample designated as control, 1, and 2 and hybridized with a probe generated from the control aliquot. The 1.0 signal obtained from the positive control indicates 100% homology between the probe and target; ratios from aliquots 1 and 2 indicate less homology between the probe and the amplicon and indicate the level of variability of V-J region sequences. There was no significant difference in the variability of the $CD4^+$ T cell V-J fragment before and after $CD4^+$ T cell depletion.

than 1 indicated less homology between the probe and the amplicon generated from different cell aliquots, suggesting a diverse content and therefore greater relative heterogeneity of V-J region sequences in these aliquots (29). For aliquots 1 and 2, the average diversity before depletion was 0.574 and 0.634, and the average diversity after depletion was 0.624 and 0.50, respectively (Figure 6). If activation and proliferation of $CD4^+$ T cells were caused by SIV-specific antigenic stimulation, the TCR repertoire would be expected to be more restricted during the time interval when elevated levels of $CD4^+Ki67^+$ T cells were noted as a result of clonal expansion. However, the absence of significant differences between the diversity of the $CD4^+$ T cell TCR V-J fragments before and after depletion suggests that in these animals, $CD4^+$ T cells are being activated in response to homeostatic stimuli induced by $CD4^+$ T cell depletion rather than by SIV-specific proliferation. While the increased $CD4^+$ T cell activation and proliferation appeared to be driven by homeostasis, the fact that the fraction of cycling $CD4^+$ T cells declined before complete reconstitution of $CD4^+$ T cell pool indicates a homeostatic failure in $CD4^+$ T cell–depleted SIV-infected SMs.

$CD4^+$ T cell depletion does not induce significant changes in the fraction of Tregs or the level of SIV-specific $CD8^+$ T cell responses. One of the primary goals of this study was to assess the contribution of $CD4^+$ T cells in controlling virus replication in naturally SIV-infected SMs. However, the observation that $CD4^+$ T cell depletion was associated with marked decline in viral load indicates that any putative role of $CD4^+$ T cells in directly controlling SIV replication is less prominent than their role as targets for the virus. However, an alternative explanation for the decline in viremia after $CD4^+$ T cell depletion is that a predominant loss of $CD4^+$ Tregs could result in expansion and/or activation of SIV-specific $CD8^+$ T cells, whose antiviral effect would then contribute to a lower set-point viremia. To test this possibility, we assessed the frequency of Tregs in peripheral blood by quantitating the fraction and number of $CD4^+FoxP3^+CD25^{hi}$ and $CD4^+CD25^{hi}CD127^{lo}$ T cells (Figure 7A) by methods previously described (30–34). No significant change in the fraction of circulating $CD4^+FoxP3^+CD25^{hi}$ T cells was noted throughout the follow-up period of study. As expected, the absolute number of $CD4^+FoxP3^+CD25^{hi}$ T cells was reduced 20 d after depletion (from 16 ± 4.52 to 2 ± 1.10 cells/mm^3) and remained at 2.5–3.9 cells/mm^3 (SD, 1.47–2.80 cells/mm^3) throughout the period of study (Figure 7B). When Tregs were defined as $CD4^+CD25^{hi}CD127^{lo}$ T cells, the fraction of this cell subset showed a transient increase in the first few weeks after depletion, while, as expected, the absolute number of $CD4^+CD25^{hi}CD127^{lo}$ T cells was reduced from 43.78 ± 30.67 cells/mm^3 (mean ± SD) before depletion to 5.12–20.76 cells/mm^3 after depletion (Figure 7B). The differences observed between $CD3^+FoxP3^+CD25^h$ T cells and $CD4^+CD25^hCD127l^{lo}$ T cells in the early stages after depletion may be related to the fact that some of the $CD4^+CD127^{lo}$ T cells could be activated $CD4^+$ T cells rather then bona fide Tregs. However, comparison of the percentage of $CD4^+CD25^{hi}CD127^{lo}$ T cells with the percentage of $CD4^+Ki67^+$ T cells did not indicate any major overlap between these cell subsets. Importantly, no correlation was found at any time point between virus replication and either the fraction or the absolute number of Tregs defined as $CD4^+FoxP3^+CD25^{hi}$ or $CD4^+CD25^{hi}CD127^{lo}$ (data not shown). Taken together, these findings indicate that it is highly unlikely that a preferential depletion of Tregs is responsible for the reduced viral load observed.

Next we sought to determine whether treatment with anti-CD4 antibody affected the level of SIV-specific $CD8^+$ T cell responses in our cohort of naturally SIV-infected SMs. To determine whether $CD4^+$ T cell depletion increased $CD8^+$ T cell responses to the virus, we measured $CD8^+$ T cell counts (Figure 2D), the fraction of activated and proliferating $CD8^+$ T cells (Figure 7C), and the level of SIV-specific $CD8^+$ T cells (Figure 7D). As previously noted, the number of $CD8^+$ T cells did not demonstrate any major changes after depletion, and there was no correlation at any time point between the fraction or number of $CD8^+$ T cells and viral load (data not shown). In addition, we found no significant changes in the fraction or absolute numbers of $CD8^+$ T cells expressing Ki67, HLA-DR, or CD69, and no correlation between the level of $CD8^+$ T cell activation or proliferation and viral load was found at any time point (data not shown). Finally, we directly assessed SIV-specific T cell responses by performing intracellular cytokine staining for IFN-γ, TNF-α, and IL-2 after stimulation of PBMCs with SIVenv and gag peptides. As shown in Figure 7D, prior to depletion, 0.29% ± 0.22% and 0.25% ± 0.19% of $CD8^+$ T cells produced IFN-γ and TNF-α, respectively, in response to each of the pools of SIV peptides. After depletion, 0.23% ± 0.15% and 0.92% ± 0.34% of $CD8^+$ T cells produced IFN-γ and TNF-α, respectively. In addition, we found no significant difference in IL-2 or CD107α expression in response to SIV peptides between samples before and after depletion (data not shown). Collectively, these findings argue against the possibility that antibody-mediated $CD4^+$ T cell depletion caused either a selective loss of Tregs or an increase in SIV-specific $CD8^+$ T cell responses in our cohort of SIV-infected SMs and thus suggest that the removal of target cells is the most likely mechanism underlying the changes in plasma viremia observed in these animals.

Discussion

Studies of the virological and immunological features of the nonpathogenic SIV infection of naturally adapted hosts, such as SMs, may allow us to gain insight into the mechanisms of AIDS pathogenesis in humans. In SIV-infected SMs, a normal or near-normal frequency and absolute number of peripheral $CD4^+$ T cells are usually maintained despite many years of infection with a highly replicating virus (6–8).

The main goal of this study was to determine how an artificially induced depletion of $CD4^+$ T cells would influence the level of

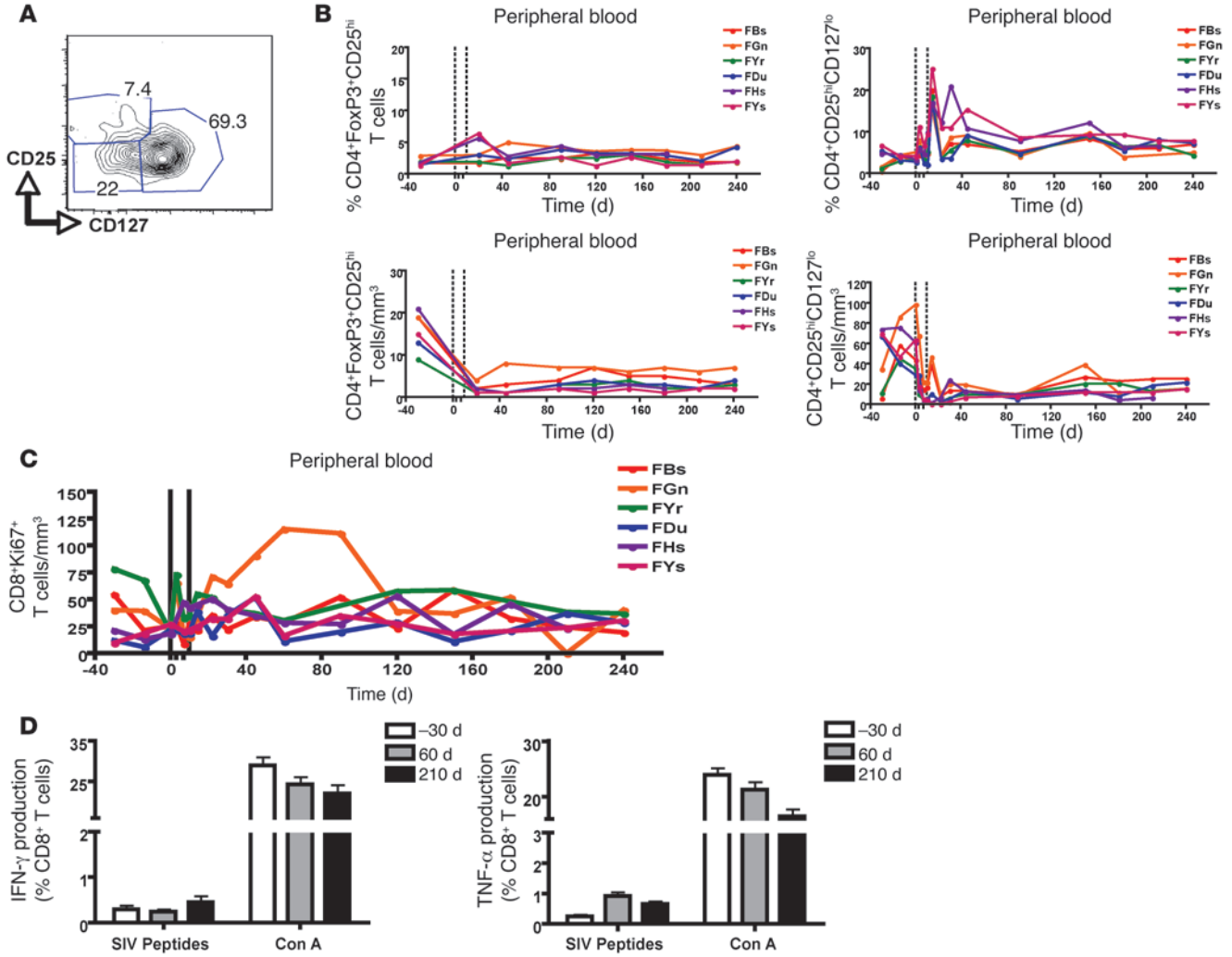

Figure 7

Longitudinal analysis of the levels of Tregs, activated CD8+ T cells, and SIV-specific CTLs during CD4+ T cell depletion. (**A**) Representative flow plot of Tregs gated as $CD25^{hi}CD127^{lo}$ (*x* axis, CD127; *y* axis, CD25; previously gated on $CD3^{+}CD4^{+}$ lymphocytes). Numbers denote percentage of cells within boxed regions. (**B**) Longitudinal assessment of the percent and absolute number of Tregs in each animal as measured by enumerating $CD4^{+}FoxP3^{+}CD25^{hi}$ T cells and $CD4^{+}CD25^{hi}CD127^{lo}$ T cells through 240 d after depletion. (**C**) Longitudinal assessment of the number of $CD8^{+}Ki67^{+}$ T cells in each animal through 240 d after depletion. Vertical lines and tick marks represent CD4-depleting antibody treatment. (**D**) Percentage of CD8+ T cells producing IFN-γ and TNF-α in response to SIV gag and env peptide pools, as measured by intracellular cytokine staining at –30, 60, and 210 d. Shown are average percent SIV-specific CD8+ T cells and CD8+ T cells that responded to the positive control (Con A). No significant changes in the level of SIV-specific CD8+ T cell responses was observed.

virus replication in naturally SIV-infected SMs. We reasoned that the key potential roles of CD4+ T cells in influencing the prevailing level of SIV replication are their helper effect on SIV-specific humoral and cellular immune responses, thus contributing to the control of virus replication, or their ability to support virus replication as preferential target cells for infection. To our knowledge, this is the first time that CD4+ T cells have been experimentally depleted during SIV infection in nonhuman primates. Our analysis of the virological and immunological effects of in vivo CD4+ T cell depletion during natural, nonpathogenic SIV infection of SMs has helped us to gain insight into the role played by these cells in this interesting animal model.

We hypothesized 3 major outcomes for this study: (a) viral load increases, indicating that a primary role for CD4+ T cells in SIV-infected SMs is to control viral replication (possibly taking place in cell lineages other than the CD4+ T cell lineage); (b) viral load decreases, consistent with the hypothesis that the main role of CD4+ T cells is to serve as a source for SIV replication, with the implication that we would expect viral load to return to the predepletion levels upon reconstitution of the CD4+ T cell pool; and (c) viral load remains stable, suggesting the absence of a major role of CD4+ T cells as either the main targets for virus replication or the cell type responsible for the immune control of viremia. We found that antibody-mediated in vivo depletion of CD4+ T cells, but not macrophages, was followed by a rapid decrease in viral load, thus suggesting that CD4+ T cells are the primary targets for viral replication in naturally SIV-infected SMs. Importantly, within a few weeks of the end of treatment we observed a rapid rebound of viremia, reaching

levels that transiently surpassed those at baseline. The decline of viremia after treatment with anti-CD4 antibody may reflect a direct effect of the antibody in blocking infection of new cells; similarly, the later rebound may reflect the clearing of the antibody from the circulation. However, we found that the rebound in viremia was temporally associated with a striking increase in the expression of markers of activation and proliferation on $CD4^+$ T cells. Even more importantly, a highly significant correlation was observed between viral load and both the absolute numbers of total and proliferating (i.e., $Ki67^+$) $CD4^+$ T cells throughout the follow-up period. These statistical analyses suggest it is highly unlikely that the kinetics of viremia we observed reflect a putative direct antiviral effect of the monoclonal antibody used. Of note, the lack of correlation between viral load and $CD4^+Ki67^+$ T cells across animals at baseline levels suggests that genetic and immunological differences between individual SMs dictate set-point levels of virus replication and activated $CD4^+$ T cells specifically for each animal.

An alternative explanation for the decline of viral load at the time of $CD4^+$ T cell depletion is that a preferential loss of Tregs results in a rapid increase in the level of SIV-specific $CD8^+$ T cell responses. However, we did not find evidence at any time point that the treatment resulted in either preferential depletion of Tregs or increased magnitude of SIV-specific $CD8^+$ T cells (defined as producing IFN-γ, TNF, or IL-2 or expressing CD107 following stimulation with SIV peptide pools), the only exception being a 3-fold increase in the fraction of TNF-α–producing cells 60 d after depletion. The observation of low cytotoxic T cell responses to the virus confirms our previous studies (13) and is consistent with the modest changes in viremia observed after $CD8^+$ cell depletion in naturally SIV-infected SMs (14). Therefore, these data further support the notion that the AIDS resistance of SMs is independent of cellular immune control of virus replication.

An interesting observation of the present study was that the depletion of $CD4^+$ T cells induced by the administered antibody persisted for much longer than the depletion of $CD8^+$ T cells obtained by similar means (i.e., infusion of a CD8-specific antibody; refs. 14, 26, 35–37). This finding is not exclusively due to the fact that the SMs included in this study were SIV infected, because a slower repopulation of $CD4^+$ compared with $CD8^+$ T cells was also observed in uninfected SMs treated with anti-CD4 antibody, although the uninfected SMs reconstituted their pool of $CD4^+$ T cells faster than the infected animals. Of note, a slow repopulation of the $CD4^+$ T cell pool after antibody-mediated depletion was also observed in an experiment conducted in HCV-infected chimpanzees (38). Therefore, our results suggest that repopulation of $CD4^+$ T cells after depletion may be intrinsically slower than that of $CD8^+$ T cells, for reasons that are still unclear but likely related to the way the homeostasis of these T cell subsets is maintained. This conclusion is consistent with studies showing that $CD4^+$ T cells repopulate much slower than do $CD8^+$ T cells after myeloablative chemotherapy and/or BM transplantation (39–45). Finally, our current findings lend some indirect support to the hypothesis that intrinsic weakness in the mechanisms regulating $CD4^+$ T cell homeostasis under depleting circumstances may play a role in the immunopathogenesis of AIDS (23, 46–48).

Theoretically, the marked increase in $CD4^+$ T cell activation and proliferation observed soon after the nadir of $CD4^+$ T cell depletion could be caused by the activation of homeostatic mechanisms aimed at repopulating the pool of $CD4^+$ T cells or by the response of SIV-specific $CD4^+$ T cells to the rapid rebound in viremia observed after the early decline. Our analysis of the TCR repertoire did not reveal any evidence of decreased TCR heterogeneity at the time of peak $CD4^+$ T cell proliferation, strongly supporting the hypothesis that this proliferation is in fact homeostasis driven, even though it fails to rapidly repopulate the pool of $CD4^+$ T cells. This conclusion is also consistent with the fact that in our cohort of naturally SIV-infected SMs, the rebound of viremia seemed to follow, rather than anticipate, the increase in $CD4^+$ T cell activation and proliferation. These findings support a model whereby the availability of activated $CD4^+$ T cells as targets for virus replication is the main determinant of the prevailing level of viremia during nonpathogenic SIV infection of a natural host species.

Intriguingly, $CD4^+$ T cell–depleted SIV-infected SMs did not experience signs of progression to AIDS despite $CD4^+$ T cell numbers that persisted up to 18 mo after depletion at levels below 100 cells/mm^3, a number that would be associated with high risk of disease progression in HIV-infected humans or SIV-infected macaques. The fact that SIV-infected SMs remain asymptomatic even when their levels of circulating $CD4^+$ T cells becomes very low has been described in previous studies of naturally SIV-infected animals (8) and in a subset of SMs that developed X4-R5 dual-tropic viruses after experimental infection (49). Collectively, these findings suggest either that SIV-infected SMs are genetically less dependent on $CD4^+$ T cells to maintain their immune system function or that, in the absence of chronic immune activation, they avoid opportunistic infections even in the context of very low $CD4^+$ T cell counts. Further studies of naturally occurring $CD4^+$ T cell–depleted and/or experimentally antibody-depleted SIV-infected SMs involving in vivo immunization with T cell–dependent antigens will be required to better characterize to what extent T helper function is dependent on $CD4^+$ T cells in SMs.

The conclusion that activated $CD4^+$ T cells support the bulk of SIV replication in SMs is consistent with our observations that in both LNs and intestinal lamina propria, the cells that are positive for SIV by in situ hybridization are $CD3^+$ and $Ki67^+$ (G. Silvestri, unpublished observations) and that the average in vivo lifespan of infected cells — as measured by the kinetics of viral load decline after treatment with antiretroviral therapy — is 1.06 d, consistent with the hypothesis that these cells are activated $CD4^+$ T cells (19). Future studies will be conducted to determine whether the amount of activated $CD4^+$ T cells is also the main determinant of viremia during pathogenic SIV infection of rhesus macaques.

The direct association of $CD4^+$ T cell counts, $CD4^+$ T cell proliferation, and virus replication in a nonpathogenic model of primate lentiviral infection described in the present study emphasizes the complexity of the relationship between HIV/SIV and the host immune system. During HIV/SIV infection, $CD4^+$ T cell proliferation may indicate the development of HIV/SIV-specific helper immune responses as well as the activation of homeostatic mechanisms directed at reconstituting the pool of $CD4^+$ T cells, both events that may protect from disease progression. However, $CD4^+$ T cell proliferation is also inextricably linked to HIV/SIV pathogenesis because it provides new targets for virus replication (11, 28). In this regard, the results of this study underscore the importance of better understanding the relationship between $CD4^+$ T cell activation and permissibility to HIV/SIV replication in order to develop therapeutic strategies in which $CD4^+$ T cell homeostasis and/or $CD4^+$ T cell responses to the virus can be enhanced without necessarily increasing the level of virus replication.

Methods

Animals. Six naturally SIV-infected SMs were used in this study. All animals were housed at the Yerkes National Primate Research Center and maintained in accordance with NIH guidelines. Animals were chosen on the criteria that they had normal $CD4^+$ T cell counts (>500 cells/mm^3). Three SMs were chosen with low viral load (<20,000 viral RNA copies/ml plasma, 1 with <120 viral RNA copies/m plasma) and 3 with high viral load (>200,000 viral RNA copies/ml plasma) in order to define a role, if any, of viral load in such depletion studies. These studies were approved by the Emory University and University of Pennsylvania Institutional Animal Care and Use Committees.

$CD4^+$ T cell depletion. A preliminary study was carried out in order to define the dose of humanized anti-CD4 mAb (Cdr-OKT4A-huIgG1; clone 12F11) that causes complete depletion of peripheral $CD4^+$ T cells in uninfected SMs. Of note, the depleting antibody used did not mask the staining with the anti-CD4 antibody (clone L200) that we used in our flow cytometric studies to assess the levels of $CD4^+$ T cells and their subsets (data not shown). Based on the results of this study, the 6 animals were treated with 10 mg/kg anti-CD4 mAb i.v. on day 0, followed by 5 mg/kg i.v. on days 3, 7, and 10. Data from preliminary experiments indicated that the antibody used persisted in the circulation for an average of 5.2–5.6 d (data not shown). Depletion efficiency in tissues other than blood (where absolute number calculation was not available) was calculated assuming that the non–$CD4^+$ T cell fraction remained unchanged by anti-CD4 antibody treatment.

Determination of plasma viral RNA. Quantitative real-time RT-PCR assay to determine SIV viral load was performed as previously described (6).

Tissue collection and processing. PBMCs were isolated by gradient centrifugation. Procedures for LN biopsy, RB, and BAL as well as isolation of lymphocytes from the obtained samples were performed as described previously (8, 20).

Immunophenotyping and flow cytometry. Multicolor flow cytometric analysis was performed on isolated cells according to standard procedures using human mAbs that were found to crossreact with SMs. Predetermined optimal concentrations of the antibodies used were as follows: anti-CD4–PerCP-Cy5.5 (clone L200; BD Biosciences — Pharmingen), anti-CD8–Alexa Fluor 700 (clone RPA-T8; BD Biosciences — Pharmingen), anti-CD3–PacBlue or –Alexa Fluor 700 (clone SP34-2; BD Biosciences — Pharmingen), anti-CD69–allophycocyanin (clone FN-50; BD Biosciences — Pharmingen), anti-CD25–allophycocyanin-Cy7 or –PE (clone M-A251; BD Biosciences — Pharmingen), anti-Ki67–FITC (clone B56; BD Biosciences — Pharmingen), anti-CD14–PE-Cy7 (clone 322A-1 [MY4]; Beckman Coulter), anti-CD127–PE (clone R34.34; Beckman Coulter), anti–HLA-DR–PE-Cy7 or –PerCPCy5.5 (clone L-243; BD Biosciences — Pharmingen), FoxP3-allophycocyanin (clone PCH101 or 236A/E7; eBioscience), and anti-Ki67–PE (clone B56; BD Biosciences — Pharmingen). Samples stained for Ki67 were fixed and permeabilized using the BD Biosciences — Pharmingen CytoFix/Perm Kit and stained intracellularly with anti-Ki67. For enumeration of Tregs, PBMCs were first surface stained with CD4-PerCP, CD25-PE, or CD127-PE and then fixed and intracellularly stained to detect FoxP3 according to the manufacturer's protocol (eBiosciences). Flow cytometric acquisition was performed on at least 100,000 events on an LSR-II cytometer driven by the FACS DiVa software (version 5.2; BD). Analysis of the acquired data was performed using FlowJo software (version 8.7.1; TreeStar). For all analysis of specific $CD4^+$ T cell subsets, we used a threshold of 200 collected events.

IHC and in situ hybridization. IHC was performed on 5-μm tissue sections mounted on Superfrost plus glass slides, dewaxed, and rehydrated in double-distilled H_2O. Antigen retrieval was performed by heating sections in 1× Diva Decloacker reagent (Biocare Medical) in a 95°C water bath for 30 min. Tissues were blocked with blocking reagent (Biocare Medical) for 1 h at room temperature. Endogenous peroxidase was blocked with 3% (v/v) H_2O_2 in TBS (pH 7.4). Primary antibodies were diluted in 10% blocking reagent in 1,3,5-trinitrobenzene and incubated overnight at 4°C. The sections were then analyzed using mouse, goat, or rabbit MACH-3 biotin-free polymer systems (Biocare Medical) according to the manufacturer's instructions and developed with 3,3′-diaminobenzidine (Vector Laboratories) or Vulcan Fast Red (Biocare Medical). Sections were counterstained with Harris (Surgipath) or CAT (Biocare Medical) hematoxylin, mounted in Permount (Fisher Scientific), and examined by light microscopy. Single in situ hybridization and double in situ hybridization plus IHC were performed as previously described (50). Antibodies used for IHC included rabbit monoclonal anti-human CD3 (SP7; Neomarkers), mouse anti-human Fascin (FCN01; Neomarkers), mouse anti-human CD68 (KP1; Dako), mouse anti-human macrophage (MAC387; Abcam), goat polyclonal anti-human CD163 (R&D Systems), mouse anti-human CD11c (5D11; Novocastra Laboratories), and mouse anti-human CD83 (1H4b; Novocastra Laboratories).

Determination of SIV antigen–specific $CD4^+$ and $CD8^+$ T cell responses. Blood samples were analyzed for SIVenv- and gag-specific immune responses using the standard intracellular cytokine assay as described previously (13).

TCR repertoire diversity. Total RNA was isolated from 3 aliquots of 50,000 highly purified $CD4^+$ T cells from a single PBMC sample (RNeasy kit; Qiagen), and cDNA was synthesized using the ProtoScript cDNA synthesis kit (New England Biolabs). TCR β-chain V-J fragment sequences were amplified using a mixture of TCRVβ and TCRJ primers. The amplification products from each of the 3 aliquots of cDNAs were purified and blotted onto a membrane. A probe labeled with α-^{32}P-dCTP was prepared from one of the amplicons (as a control) by PCR, hybridized to each dilution of the membrane-immobilized aliquots of amplicons from the control and each dilution of the other 2 aliquots. Hybridization signals were quantitated by densitometry. TCR diversity was calculated as the ratio of the hybridization signals obtained from each aliquot derived from the same $CD4^+$ T cell donor to the signal obtained from the positive control (DNA aliquot from which the probe was made). The signal obtained from the positive control ratio was denoted as 1 (i.e., 100% homology between the probe and target); ratios that gave values less than 1 indicated decreasing levels of homology between the probe and the amplicon generated from different cell aliquots.

Statistics. Spearman and Pearson correlation tests were performed on all samples, using mean, SD, and sample count. All statistical analysis was performed using Prism (version 4.0C; GraphPad Software Inc.) or SAS 9.1 (SAS Institute Inc.) software. Random effects models were used to estimate the influence of time and animal on $CD4^+$ versus $CD4^+Ki67^+$ T cell counts and log viral loads. Partial correlations were then computed between $CD4^+$ and $CD4^+Ki67^+$ counts and for log viral loads adjusted for time and animals. Random effects models allow for estimation of these influences on the number of $CD4^+Ki67^+$ T cells and viral loads separately, with nonlinear effects for time. Therefore, correlations can be computed between the residuals from the 2 random effects models to provide a partial correlation between $CD4^+Ki67^+$ T cells/mm^3 and log viral load. While Spearman and Pearson correlations were also used to determine correlations between these values, and a significant correlation was found between the number of activated T cells and viral load, these analyses are limited because they only account for the relationship between measurements on any given day. The partial correlation analysis is more appropriate for this study because this method takes into account the longitudinal structure (and hence serial correlation) inherent in the data and provides a single estimate for the relationship between activation and viral load over all measurements. A *P* value less than 0.05 was considered significant.

Acknowledgments

We acknowledge Stephanie Ehnert and all the animal care and veterinary staff at the Yerkes National Primate Research Center, the Virology Core of the Emory Center for AIDS Research (CFAR),

and the NIH nonhuman primate reagent resource. In addition, we would like to thank Ann Chahroudi for critical review of this manuscript. This work was supported by NIH grants R01-AI66998 and R01-HL-75766 (to G. Silvestri), R01-AI27057 (to A.A. Ansari), R21-AI060451 (to D.L. Sodora), R24RR16988 (to F. Villinger), and RR-00165 (to the Yerkes National Primate Research Center). The CD4-depleting antibody used in this study was provided by the NIH Nonhuman Primate Reagent Resource supported by NIH grants RR016001 and AI040101.

Address correspondence to: Guido Silvestri, Department of Pathology and Laboratory Medicine, University of Pennsylvania School of Medicine, 705 Stellar Chance Laboratories, 422 Curie Blvd., Philadelphia, Pennsylvania 19104, USA. Phone: (215) 573-5363; Fax: (215) 573-5369; E-mail: gsilvest@mail.med.upenn.edu. Or to: Aftab A. Ansari, Department of Pathology and Laboratory Medicine, Emory University School of Medicine, 2309 WMB, 101 Woodruff Circle, Atlanta, Georgia 30321, USA. Phone: (404) 712-2834; Fax: (404) 712-1771; E-mail: pathaaa@emory.edu.

Received for publication September 4, 2007, and accepted in revised form March 21, 2008.

Donald L. Sodora's present address is: Seattle Biomedical Research Institute, Seattle, Washington, USA.

1. Hahn, B.H., Shaw, G.M., De Cock, K.M., and Sharp, P.M. 2000. AIDS as a zoonosis: scientific and public health implications. *Science.* **287**:607–614.
2. Gao, F., et al. 1992. Human infection by genetically diverse SIVSM-related HIV-2 in west Africa. *Nature.* **358**:495–499.
3. Johnson, P.R., and Hirsch, V.M. 1991. Pathogenesis of AIDS: the non-human primate model. *AIDS.* **5**(Suppl. 2):S43–S48.
4. Apetrei, C., et al. 2005. Molecular epidemiology of simian immunodeficiency virus SIVsm in U.S. primate centers unravels the origin of SIVmac and SIVstm. *J. Virol.* **79**:8991–9005.
5. VandeWoude, S., and Apetrei, C. 2006. Going wild: lessons from naturally occurring T-lymphotropic lentiviruses. *Clin. Microbiol. Rev.* **19**:728–762.
6. Silvestri, G., et al. 2003. Nonpathogenic SIV infection of sooty mangabeys is characterized by limited bystander immunopathology despite chronic high-level viremia. *Immunity.* **18**:441–452.
7. Chakrabarti, L.A., et al. 2000. Normal T-cell turnover in sooty mangabeys harboring active simian immunodeficiency virus infection. *J. Virol.* **74**:1209–1223.
8. Sumpter, B., et al. 2007. Correlates of preserved CD4(+) T cell homeostasis during natural, non-pathogenic simian immunodeficiency virus infection of sooty mangabeys: implications for AIDS pathogenesis. *J. Immunol.* **178**:1680–1691.
9. Rey-Cuille, M.A., et al. 1998. Simian immunodeficiency virus replicates to high levels in sooty mangabeys without inducing disease. *J. Virol.* **72**:3872–3886.
10. Ling, B., et al. 2004. Classic AIDS in a sooty mangabey after an 18-year natural infection. *J. Virol.* **78**:8902–8908.
11. Stevenson, M. 2003. HIV-1 pathogenesis. *Nat. Med.* **9**:853–860.
12. Stebbing, J., Gazzard, B., and Douek, D.C. 2004. Where does HIV live? *N. Engl. J. Med.* **350**:1872–1880.
13. Dunham, R., et al. 2006. The AIDS resistance of naturally SIV-infected sooty mangabeys is independent of cellular immunity to the virus. *Blood.* **108**:209–217.
14. Barry, A.P., et al. 2007. Depletion of CD8+ cells in sooty mangabey monkeys naturally infected with simian immunodeficiency virus reveals limited role for immune control of virus replication in a natural host species. *J. Immunol.* **178**:8002–8012.
15. Wei, X., et al. 1995. Viral dynamics in human immunodeficiency virus type 1 infection. *Nature.* **373**:117–122.
16. Ho, D.D., et al. 1995. Rapid turnover of plasma virions and CD4 lymphocytes in HIV-1 infection. *Nature.* **373**:123–126.
17. Perelson, A.S., Neumann, A.U., Markowitz, M., Leonard, J.M., and Ho, D.D. 1996. HIV-1 dynamics in vivo: virion clearance rate, infected cell life-span, and viral generation time. *Science.* **271**:1582–1586.
18. Nowak, M.A., et al. 1997. Viral dynamics of primary viremia and antiretroviral therapy in simian immunodeficiency virus infection. *J. Virol.* **71**:7518–7525.
19. Gordon, S.N. et al. 2008. Short-lived infected cells support virus replication in sooty mangabeys naturally infected with simian immunodeficiency virus: implications for AIDS pathogenesis. *J. Virol.* **82**:3725–3735.
20. Gordon, S.N., et al. 2007. Severe depletion of mucosal CD4+ T cells in AIDS-free simian immunodeficiency virus-infected sooty mangabeys. *J. Immunol.* **179**:3026–3034.
21. Paiardini, M., et al. 2006. Perturbations of cell cycle control in T cells contribute to the different outcomes of simian immunodeficiency virus infection in rhesus macaques and sooty mangabeys. *J. Virol.* **80**:634–642.
22. Fauci, A.S., Pantaleo, G., Stanley, S., and Weissman, D. 1996. Immunopathogenic mechanisms of HIV infection. *Ann. Intern. Med.* **124**:654–663.
23. McCune, J.M. 2001. The dynamics of CD4+ T-cell depletion in HIV disease. *Nature.* **410**:974–979.
24. Picker, L.J. 2006. Immunopathogenesis of acute AIDS virus infection. *Curr. Opin. Immunol.* **18**:399–405.
25. Schmitz, J.E., et al. 1999. Control of viremia in simian immunodeficiency virus infection by CD8+ lymphocytes. *Science.* **283**:857–860.
26. Jin, X., et al. 1999. Dramatic rise in plasma viremia after CD8(+) T cell depletion in simian immunodeficiency virus-infected macaques. *J. Exp. Med.* **189**:991–998.
27. Lifson, J.D., et al. 2001. Role of CD8(+) lymphocytes in control of simian immunodeficiency virus infection and resistance to rechallenge after transient early antiretroviral treatment. *J. Virol.* **75**:10187–10199.
28. Finzi, D., and Siliciano, R.F. 1998. Viral dynamics in HIV-1 infection. *Cell.* **93**:665–671.
29. Naylor, K., et al. 2005. The influence of age on T cell generation and TCR diversity. *J. Immunol.* **174**:7446–7452.
30. Hori, S., Nomura, T., and Sakaguchi, S. 2003. Control of regulatory T cell development by the transcription factor Foxp3. *Science.* **299**:1057–1061.
31. Hartigan-O'Connor, D.J., Poon, C., Sinclair, E., and McCune, J.M. 2007. Human CD4+ regulatory T cells express lower levels of the IL-7 receptor alpha chain (CD127), allowing consistent identification and sorting of live cells. *J. Immunol. Methods.* **319**:41–52.
32. Liu, W., et al. 2006. CD127 expression inversely correlates with FoxP3 and suppressive function of human CD4+ T reg cells. *J. Exp. Med.* **203**:1701–1711.
33. Seddiki, N., et al. 2006. Expression of interleukin (IL)-2 and IL-7 receptors discriminates between human regulatory and activated T cells. *J. Exp. Med.* **203**:1693–1700.
34. Pereira, L.E., et al. 2007. Simian immunodeficiency virus (SIV) infection influences the level and function of regulatory T cells in SIV-infected rhesus macaques but not SIV-infected sooty mangabeys. *J. Virol.* **81**:4445–4456.
35. Schmitz, J.E., et al. 2005. Effect of CD8+ lymphocyte depletion on virus containment after simian immunodeficiency virus SIVmac251 challenge of live attenuated SIVmac239delta3-vaccinated rhesus macaques. *J. Virol.* **79**:8131–8141.
36. Matano, T., et al. 1998. Administration of an anti-CD8 monoclonal antibody interferes with the clearance of chimeric simian/human immunodeficiency virus during primary infections of rhesus macaques. *J. Virol.* **72**:164–169.
37. Lifson, J.D., et al. 2003. Transient early post-inoculation anti-retroviral treatment facilitates controlled infection with sparing of CD4+ T cells in gut-associated lymphoid tissues in SIVmac239-infected rhesus macaques, but not resistance to rechallenge. *J. Med. Primatol.* **32**:201–210.
38. Grakoui, A., et al. 2003. HCV persistence and immune evasion in the absence of memory T cell help. *Science.* **302**:659–662.
39. Velardi, A., et al. 1988. Imbalances within the peripheral blood T-helper (CD4+) and T-suppressor (CD8+) cell populations in the reconstitution phase after human bone marrow transplantation. *Blood.* **71**:1196–1200.
40. Mackall, C.L., et al. 1995. Age, thymopoiesis, and CD4+ T-lymphocyte regeneration after intensive chemotherapy. *N. Engl. J. Med.* **332**:143–149.
41. Kook, H., et al. 1996. Reconstruction of the immune system after unrelated or partially matched T-cell-depleted bone marrow transplantation in children: immunophenotypic analysis and factors affecting the speed of recovery. *Blood.* **88**:1089–1097.
42. Roux, E., et al. 2000. Recovery of immune reactivity after T-cell-depleted bone marrow transplantation depends on thymic activity. *Blood.* **96**:2299–2303.
43. Storek, J., et al. 2001. Immune reconstitution after allogeneic marrow transplantation compared with blood stem cell transplantation. *Blood.* **97**:3380–3389.
44. Fujimaki, K., et al. 2001. Immune reconstitution assessed during five years after allogeneic bone marrow transplantation. *Bone Marrow Transplant.* **27**:1275–1281.
45. Mohty, M., et al. 2002. Recovery of lymphocyte and dendritic cell subsets following reduced intensity allogeneic bone marrow transplantation. *Hematology.* **7**:157–164.
46. Margolick, J.B., et al. 1998. Decline in total T cell count is associated with onset of AIDS, independent of CD4(+) lymphocyte count: implications for AIDS pathogenesis. *Clin. Immunol. Immunopathol.* **88**:256–263.
47. Silvestri, G., and Feinberg, M.B. 2003. Turnover of lymphocytes and conceptual paradigms in HIV infection. *J. Clin. Invest.* **112**:821–824.
48. Grossman, Z., Meier-Schellersheim, M., Sousa, A.E., Victorino, R.M., and Paul, W.E. 2002. CD4+ T-cell depletion in HIV infection: are we closer to understanding the cause? *Nat. Med.* **8**:319–323.
49. Milush, J.M., et al. 2007. Virally induced CD4+ T cell depletion is not sufficient to induce AIDS in a natural host. *J. Immunol.* **179**:3047–3056.
50. Li, Q., et al. 2005. Peak SIV replication in resting memory CD4+ T cells depletes gut lamina propria CD4+ T cells. *Nature.* **434**:1148–1152.